Available online at www.sciencedirect.com

ScienceDirect

Procedia Structural Integrity 3 (2017) 432–440

Structural Integrity Procedia

www.elsevier.com/locate/procedia

XXIV Italian Group of Fracture Conference, 1-3 March 2017, Urbino, Italy

Determination of critical stress in high strength concrete

A. D'Aveni[1], G. Fargione[1], E. Gugliemino[2], G. Risitano[2,*], A. Risitano[3]

[1]*Department of Civil Engineering and Architecture, University of Catania, Viale A, Doria 6 95125 Catania Italy*

[2]*Department of Engineering, University of Messina, Messina, Italy*

[3]*C.R.P.S., Catania, Italy*

Abstract

In this work, more specimens were tested at equal conditions (static compression test) and, during the tests, the released heat for irreversible phenomena was monitored by means of the analysis of the temperature surface of the specimen. In this way, it was possible to estimate the average value of the macroscopic stress ("critical stress") for which local micro cracks begin.
The compression static tests (load - machine time) and the related thermal analysis (temperature-machine time) of spots located on the specimen face of the specimens, highlighted the possibility to estimate the value of the compressive load to which there was loss of linearity in the temperature - machine time diagram (Δt-t). This effect is due to internal heat generated for irreversible phenomena (internal micro fractures).
The results show that the "critical stress" has values practically coincident for the points (spots) located in different zones (center or corners of the specimens' surface).

Peer-review under responsibility of the Scientific Committee of IGF Ex-Co.

Keywords: crack; stress limit; concrete; temperature-test; fatigue.

1. Introduction

The fatigue characterization of high strength concrete is a problem that in recent years has aroused more and more interest in the scientific community sector (fracture mechanics). The technical literature on the subject is full of proposals for methods. In Susmel (2014) and Jadallah et al. (2016) the authors propose an interesting calculus model

* Corresponding author. Tel.: +39 347 3209239.
E-mail address: giacomo.risitano@unime.it

Peer-review under responsibility of the Scientific Committee of IGF Ex-Co.
10.1016/j.prostr.2017.04.067

and an extensive bibliography that highlights the efforts of researchers on this field. As a result of events that may be related to inadequate knowledge of the fatigue strength of concrete structures, the literature has proposed many scientific works that suggest more effective methods of investigation and formulations to evaluate the fatigue limit of concrete. The uncertainty related to the causes of collapse of reinforced concrete structures subjected to dynamic loads, that occurred after long years of activity, suggests, as another additional cause, the decay of fatigue performances of the concrete.

Nowadays, as well as new experimental methods for fatigue characterization of concrete are adopted, are also proposed mathematical models based on fracture mechanics theory by Bazant and Hubler (2014), Bazant and Al. (1983). These models are based on the assumption that the cause of rupture is due to the growth of micro fractures already present in the material at the time of implementation. They conclude that the amplitude (w) of the micro fracture is a function (less than a constant) of the fourth power of the stress ($w= k\ \sigma^4$) and so, the achievement of critical conditions is particularly fast. The tests methods adopted for the determination of the "critical stress" of the concrete, reproduce those normalized and encoded used for other materials (steels, composite, etc.). Thomas et Al. (2014), Hoover et Al. (2013) as, for example, the 4-point bending test of beam element by Charalambidi et Al. (2016) in which more easily adequate stress values can be reached under dynamic loads. Instead, the classical fatigue tests on high strength concrete cubes, equal to those used for standard static tests, involve the use of fatigue machines equipped with actuators of significant powers, not always easy to have, and in addition not indifferent time tests for the definition of the classic fatigue limit.

According to the experience of the authors in the field of metallic materials Risitano A. and Risitano G. (2013), Fargione et Al. (2014) and of other researchers in the field of composites like Colombo et Al. (2012) and Crupi et Al. (2015), in the use of energetic methods for the determination of the critical stress of materials, a similar procedure can be used successfully also for the concrete. This procedure, based on the analysis of temperature caused by released heat for irreversible phenomena under stress, allows to determine the "critical stress" σ_L for high-strength concretes such as those that can be used in the construction of viaducts, bridges and airport runways. These, notoriously, are subjected to dynamic loads during their useful life. The expense in time and in equipment that involves the classical fatigue testing of concrete does not allow, in technical practice, the fatigue characterization. The maximum stress assumed, according to SLS Italian code (NTC 2008), defines the elastic limit valid for structural analysis purposes, and not the possible fatigue limit of the material, remaining thus uncertainty in the real possibilities of concrete strength to dynamic loads. Accordingly, the authors are convinced that it is convenient to refer to energy methods in which, for example, the temperature becomes an indicative parameter of the lost energy in the material.

The procedure to evaluate, by energetic methods, the "stress limit" σ_L of high-strength concrete was used by the authors in a previous work Risitano et Al. (2016). In this work, a more significant number of specimen (14) of the same mix design and equal shape has allowed to validate statistically what previously obtained. In addition, it has permitted to assert that the maximum assumed stress of the concrete, under the quasi-permanent combination load ($\sigma_{max} \leq 0{,}45\ f_{ck}$), fixed by the Italian code NTC 2008, appears to be protective compared to the fatigue limit. The proposed procedure allows also to define the value of the allowable stress in the range (0,45 to 0,60 f_{ck}) at the serviceability limit state (SLS), according to Italian code NTC2008 and advantages also in terms of safety for the structures and for the most appropriate choices during the design phase.

Nomenclature

w	amplitude of the micro fracture
σ_L	"critical stress"
R_c	cubic strength of concrete
σ_Y	stress yield
K_m	thermoelastic coefficient
σ_m	monoaxial normal stress (load/area)
σ	generic normal stress
T_0	specimen temperature [K]
ΔT	surface specimen temperature variation

t	time test [s]
c_v	specific heat at constant volume
B	coefficient depending from the characteristics of the material
ν	Poisson coefficient

2. Physical background

As already described by Risitano et Al. (2016), the procedure applied for the fatigue characterization of the concrete, is based on the thermoelastic heat released by solids under stress. This effect was applied to homogeneous solids by Lord Kelvin, who defined the law of variation of the temperature in adiabatic conditions, under mechanical mono axial stress, as follows:

$$\Delta T = K_m T_0 \sigma_m \tag{1}$$

The thermoelastic phenomenon has recently been analyzed and experimentally verified by Gaglioti et Al. (1983). They, by means of mono axial load tests on the steel material, have derived the diagram temperature – machine time (ΔT-t), in order to derive the stress yield of the material. They identified that the "stress yield" σ_y was in correspondence with the horizontal tangent of the diagram in figure 1.

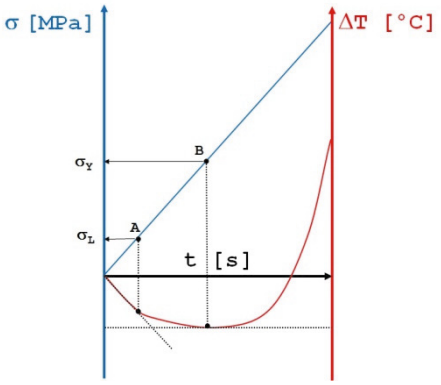

Fig. 1. Qualitative ΔT vs time trend.

The evaluation of the released heat during the loading of the steel material has been addressed in more detail also by Melvin et Al. (1990) and Melvin et Al. (1993). For the above mentioned authors, the formation of micro cracks in the specimen results in the loss of linearity in the temperature – machine time diagram (ΔT-t) that, after a first part with a linear trend assumed a higher order trend with increasing of temperature values up to a maximum (horizontal tangent) to continue with gradient reversal (figure 1).
They starting from the thermodynamic theory and evaluating the entropy as the sum of thermodynamic forces and fluxes, write the equation of the temperature as Melvin et Al. (1990):

$$\partial T / \partial t - \chi \nabla 2T = -\gamma \frac{T_0}{E}(1-2\nu)\frac{d\sigma}{dt} \tag{2}$$

For simple tensile-compressive stress and homogeneous materials, assuming a constant stress rate high enough to assure an adiabatic behaviour but not enough to neglect the viscous effects, the equation (2) takes the form:

$$\Delta T = K_m T_0 \sigma_m - B\sigma^2{}_m / \left(3C_v E\right) \quad (3)$$

In this equation, ΔT is the temperature variation of the specimen during the test, K_m and B (see Melvin et Al. (1990)) are coefficients that for metals and concrete are negative, σ_m is the applied stress, c_v is the specific heat at constant volume per unit volume and E is the elastic modulus of the material. The second term of the equation (3) describes the non-linearity of the diagram of Figure 1 and assumes significant values when plastic deformations in the material occur.

The mathematical modelling is not easy to apply in practical cases for the uncertainty in the assessment of coefficients. It is easy to implement the experimental analysis because, nowadays, high precision sensors are available, sensors which able to read centesimal variations of the temperature surface. The use of high precision instrumentation allows to have, experimentally, the temperature – machine time diagram *(ΔT-t*) during the loading process, and permits to define, on the diagram, the point at which the linearity defined by $k_m T_0 \sigma_m$ term ends.

The authors consider of great scientific interest the study of the part of the load - temperature - time machine diagram (*P-ΔT-t*), (A-B) part in figure 1, where the tangent changes continuously for the effect of $B\sigma_m^2/(3c_vE)$ term of (3), because this part is linked to the fatigue time diagram of the material.

It is known that the fatigue failure of a material (in dynamic test) begins for the stress value that determines the first micro-plasticity in the material. The area of micro plasticity, under repeated loads, increases up to produce cracks and consequent failure. It is realistic to assume that the load, that applied in a static way produces micro-plasticity at a local level, will lead to the failure of the material when it is applied in a cyclic way.

Through the identification of the first loss of linearity in the temperature–machine time diagram (*ΔT-t*) is possible to determine the stress which has caused it and, therefore, the possible "critical stress".

It's important to emphasize that, in a static loading process, the range values of stresses corresponding to the no linear portion of the diagram *(ΔT-t*), limited in the bottom by the horizontal tangent (figure 1), are all values of the fatigue time curve (Wohler diagram)

In the case of concrete specimens, although the homogeneity of the material is not realistic, the first tests Risitano et Al. (2016) have shown that important indications on the fatigue problem of the concrete could be deduced. In particular, it has been possible to identify the first change of slope in the temperature–machine time diagram (*ΔT-t*) during the static loading process. The first change of the slope defines a situation of heat input that is different from the one defined by the perfect thermo-elasticity equation (first member of the (3)) and, correspondently, indicates the "critical stress" σ_L. Loads (or stresses) even slightly higher than this value, can lead to the failure of the material, when they are applied in fatigue way.

3. Material and methods

The tests were performed on concrete cubic specimens of 15 cm side, whose mix design per cubic meter is: a) inert for 1820 daN (4-16 size for 25%, 0-4 size for 65%, 0-2 size for 10%); b) cement CEM I 52.5 R for 410 daN; c) water for 172 litres; d) additive MAPEI "Dynamon NSG 1022" for 3.5 litres. The concrete has density: 2404 kg / m^3, slamp tests: 210 cm, class of consistency: S4.

Static strength has been obtained with the test machine: CONTROLS, cat: C7600, series: 08.006.660, capacity: 5000 kN, year: 2008 Applied load: 1Mpa/s. The tests were carried out in load control with constant speed (N/s). The thermal images have been acquired by thermal infrared Camera: FLIR SC300.

Figure 2a, shows a concrete specimen loaded in a uniaxial compression static way, with near the thermal image of a specimen surface at the beginning of the test (figure 2b). This image identifies the survey points/zones (spots/square) and helps to detect the reference temperature of the tests (image zero).

The five detection points (spots, areas) are situated as in figure 2b. They are the references to define the temperature trend during the execution of the tests and are aligned along the diagonals, with spot 5 positioned at the center of the exposed surface. The acquisition frequency of the images was of 10 Hz.

The following figures (3a, 3b) show the thermal images in two distinct moments of the tests, at the application of about 70% of the ultimate load (Fig. 3a) and immediately before failure (Fig. 3b), respectively. In the images are clearly visible the zones of the surface specimen mostly stressed (for possible positioning defects and/or for load leveling) and then at higher temperatures.

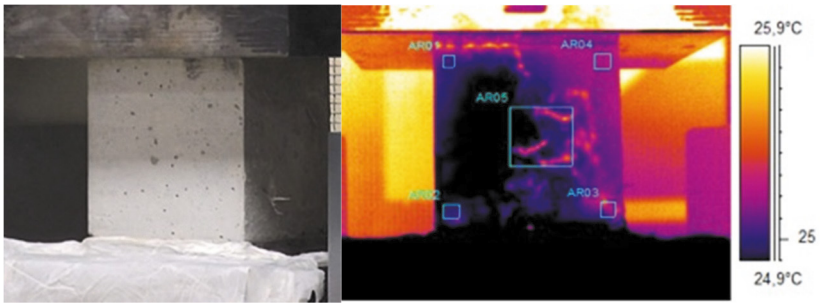

(a) (b)

Fig. 2. (a) adopted specimen; (b) Thermal image of one face at the beginning of the test with the analysed zones (square).

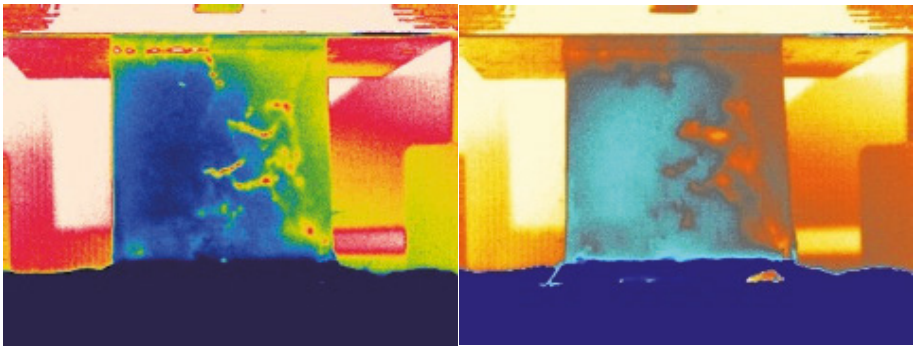

(a) (b)

Fig.3. (a) thermal image of a face of the specimen at 70% of the ultimate load; (b) close to the ultimate load.

4. Results and analysis

As stated in the previous work (Risitano et Al. (2016)), the thermal diagrams acquired during the static compression tests are used to define:

1) A first phase in which at the variation of the internal stress of the specimen, the thermoelastic characteristic is well represented by an interpolating straight line. The behaviour of the material is practically homogenous and locally there are no micro cracks. In this phase, the second term of equation (3) is practically irrelevant;
2) A second phase in which the interpolating curve may be approximated with a broken line. The first change of slope of the broken line, that approximates the second part of the curve, is due to reaching of a stress value such as to produce the first micro-failures in the internal structure of the specimen. In this phase, the specimens release heat for plastic deformation and/or for internal flows between aggregates and cement and/or between aggregates and aggregates. Correspondingly, the second term of equation (3), by increasing the applied load, becomes more and more important with a high increasing of temperature immediately before the specimens failure.

The Figure 4 shows the points data of one of the 14 specimens subjected to uniaxial compression static test. In the diagram, in addition to the data temperature points versus time machine, are reported their moving average (20 points) and the applied load. The two straight lines (in black) of the diagram define: one the thermoelastic part (first straight line), the other the part with heat input for irreversible phenomena (second straight line). In the diagram the intersection point of the two straight lines and the corresponding load of 1050 kN ("critical load") for which the

thermoelastic phase is to consider exhausted, are defined.

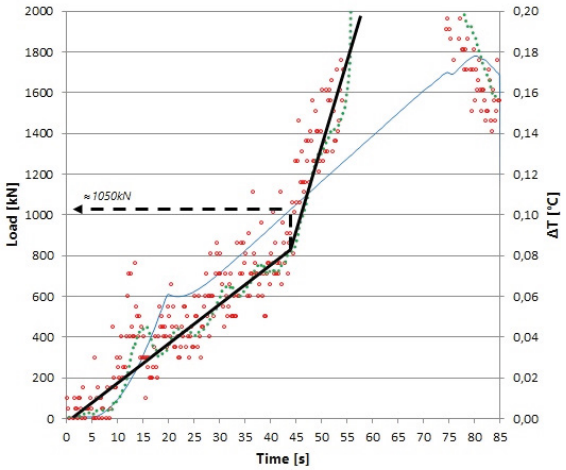

Fig. 4. ΔT vs time curve (red points) and stress vs time curve (blue line) for spot number 5.

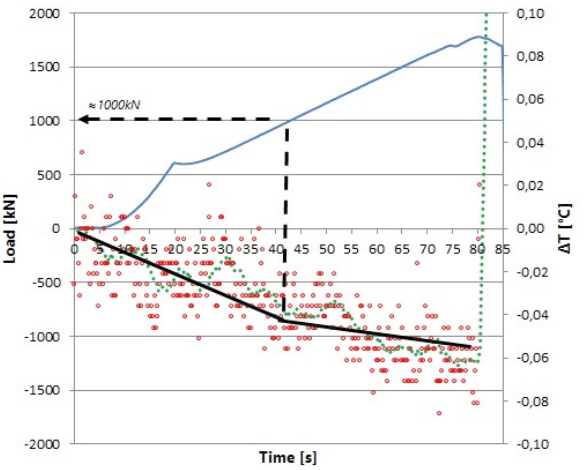

Fig. 5. ΔT vs time curve (red points) and stress vs time curve (blue line) for spot number 4.

The Figure 5 refers to the spot located on a corner of the same specimen. In it is reported the trend of the temperature that, unlike what occurred for the central spot, decreases with continuity up to a value in which it is possible to define, even if it is in a less evident than occurs in the previous central spot the change of the slope. The figure 6a, that is related to the thermal image immediately before the breakage of the specimen, shows the distribution of temperatures near a corner which, as it is known, is completely different from the one found on the center spot. This is due to the plate of the testing machine that activates a distorted tensional state. Despite the plate machine effect detectable in the corner spot, the value of the critical load defined as the intersections point of two interpolating straight lines, is equal to about 1000 kN and so practically comparable with the one recorded on the central spot (spot 5).

In all the examined specimens, it was observed a trend of temperature data similar to the one already described. In all specimens, it can be clearly identified the value of the load of the first change of slope of the interpolating line the points detected by the thermography camera. From these points, it was easy to read on the load diagram, the critical load and the related "critical stress".

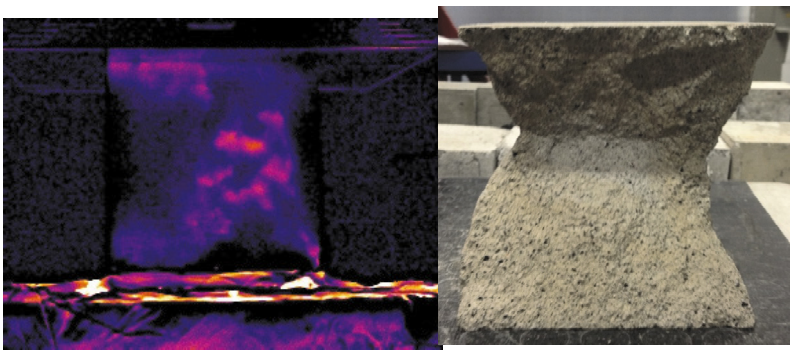

Fig. 6. (a) thermal image of the specimen at the failure; (b) hourglass shape of the specimen at the failure.

The assessment of the critical load was performed with reference to the spot positioned at the centre (spot 5) of all specimens where the plate machine effect was almost absent and the temperature variations were better comparable due to their better homogeneity. However, the temperature data detected on the corner that first showed signs of failure, were used as result comparison.

The load data, the variation of temperature and the machine time, shown in the diagrams, were coordinated among

them taking as common reference the instant of rupture of the specimen. In fact, due to the tolerances between the two plates of the testing machine and the surfaces of the specimen, in the first part of load application, it was not easy to define a clear coordination of the recorded data (change in temperature, load on the specimen). This is clearly visible in the diagrams of figures 4, 5.
The results of the measurements carried out on all specimens have been reported in Table 1. In it, the first column shows the reference number of the specimen, in the second column the value of resistance R_c [MPa] of the specimen, in the third column, the "critical stress" σ_L [MPa] referring to the centre spot and that of the corner spot, and in the fourth column their ratio $r = \sigma_L/R_c$. referring to the centre spot and that of the corner spot.

Table 1. cubic strength of concrete R_c and "critical stress" σ_L (fatigue) of the concrete.

Specimen	cubic strength of concrete R_c [MPa]	"critical stress" σ_L [MPa]		$r = \sigma_L / R_c$	
		Center	Corner	Center	Corner
1	82	45	43	0.55	0.52
2	77	54	46	0.70	0.60
3	88	68	58	0.77	0.66
4	79	51	46	0.64	0.58
5	84	47	53	0.55	0.63
6	79	47	44	0.59	0.56
7	84	43	44	0.51	0.53
8	73	52	53	0.72	0.73
9	101	60	38	0.60	0.38
10	80	51	53	0.64	0.67
11	89	49	36	0.55	0.40
12	84	47	42	0.55	0.50
13	82	31	40	0.38	0.49
14	82	53	42	0.65	0.51
Average (R_c)	83	50	45	0.60	0.55
Dev. St.	6.6	8.4	6.6	0.098	0.010

The examination of the images of all specimens shows the possibility to identify the lines along which the material will begin to fail locally and this for a much lower load than that of the breaking load of the specimen. The areas where the "critical stress" of the material exceeded, are highlighted with colour stains to indicate different local temperatures: see, for example, between the centre and the corner of the specimen surface. Finally, at all field the thermal images detectable during the load application show that, as approaching the stress the stress yield of the material, the temperature lines become more marked giving indications of possible start of cracks within the specimen, as is well shown in figures 3 and 6a.
In summary, the thermoelastic effect is perfectly visible and it is perfectly identifiable the instant of loss of linearity in the (ΔT- t), diagram to which corresponds the "critical stress" on the related (P-t) diagram. The temperature deviates from the straight line for a load to which corresponds a stress equal to 49.8 MPa (average of values relative to the central spot) equal to about 60% of the resistance to the concrete failure.

Conclusions

Further compression static tests on high strength concrete cubic specimens of side 15 cm were performed to

determine, on a more significant sample, the "critical stress" defined as the macroscopic stress (load/area of the section) [Mpa] for which, within the concrete material, irreversible phenomena (nonlinear) begin.
The application of the static load, according to a protocol already established for homogeneous materials (steel) from Risitano A. and Risitano G. (2013), Risitano et Al. (2012), Fargione et Al. (2013), Fargione et Al. (2014), Colombo et Al (2012), highlights that:

A. It is possible to identify, during the tests and on the exposed face of the specimen, points of maximum stress that will produce local cracking also much before reaching the breaking load of the specimen (50% -70% of the rupture load);
B. The evolution of the non-linearity, also at a local level, can be attended during the tests and the average stress σ_L (load/area of the section) which determines the beginning can give indications on the "critical stress" of concrete;

On the basis of these results, it is confirmed that:

1. A suitable protocol test may be adopted, both in the testing stage and in the working stage, as a non-destructive method for determining the "critical stress" of concrete structures.
2. The current Italian code NTC 2008 (paragraph 4.1.2.2.5.1) for concrete, which identifies for the serviceability state limit (SLS) the normal stress $\sigma_{max} \leq (0.45 \text{ to } 0.60)\, f_{ck}$, seems to be precautionary. According to the procedure proposed in this paper, by means of static uniaxial compression test, it is possible to define the allowable characteristic cylindrical stress of the legal field values (0.45 to $0.60\, f_{ck}$) in a more accurate way.

Future research programs of the authors contemplate classic fatigue tests (tests with dynamic load machines) in order to verify that the compression fatigue limit of the material is consistent with the "critical stress" obtained with uniaxial static compression tests.

Acknowledgement

Thanks for the supply of concrete specimens to I.C.E.A. companies LTD - Industry and premixed concrete - S.P. n. 3 km 0:30 - Zona Industriale Piano Tavola 95032 Belpasso (CT)

References

Bazant, Z.P., Hubler, V., 2014. Theory of cyclic creep of concrete based on Paris law for fatigue growth of subcritical microcracks. Journal of the Mechanics and Physics of Solids 63, 187–200.
Bažant, Z.P., Oh, B.H., 1983. Crack band theory for fracture of concrete. Materials and structures 16, 155–177.
Charalambidi, B.G., Rousakis, T.C., Karabinis, A.I., 2016. Analysis of the fatigue behavior of reinforced concrete beams strengthened in flexure with fiber reinforced polymer laminates. Composites Part B: Engineering 96, 69–78.
Charalambidi, B.G., Rousakis, T.C., Karabinis, A.I., 2016. Fatigue Behavior of Large-Scale Reinforced Concrete Beams Strengthened in Flexure with Fiber-Reinforced Polymer Laminates. Journal of Composites for Construction 20.
Colombo, C., Vergani, L., Burman, M., 2012. Static and fatigue characterisation of new basalt fibre reinforced composite. Composite Structures 94, 1165–1174.
Crupi, V., Guglielmino, E., Risitano, G., Tavilla, F., 2015. Experimental analyses of SFRP material under static and fatigue loading by means of thermographic and DIC techniques. Composites Part B: Engineering 77, 268-277.
Fargione, G., Risitano, A., Guglielmino, E., 2014. Definition of the linearity loss of the surface temperature in static tensile test. Frattura ed Integrità Strutturale 30, 201-210.
Fargione, G., Risitano, G., Tringali, D., Guglielmino, E., 2013. Fatigue characterization of mechanical components in service. Frattura ed Integrità Strutturale 26, 143-155.
Gaglioti, G., 1982. Mechanical and thermal behaviour of metallic materials. G. Caglioti and A. Ferro Editors, Amsterdam.
Hoover, C.G., Bažant, Z.P., Vorel, J., Wendner, R., Hubler, M.H., 2013. Comprehensive concrete fracture tests: Description and results. Engineering Fracture Mechanics 114, 92–103.
Jadallah, O., Bagni, C., Askes, H., Susmel, L., 2016. Microstructural length scale parameters to model the high-cycle fatigue behaviour of notched plain concrete. International Journal of Fatigue 82, 708–720
Melvin, A.D., Lucia, A.C., Solomos, G., Volta, G., Emmony, D.C., 1990. Thermal emission measurements from creep damaged specimens of AISI 316L and Alloy 800H, DC Emmony 9th International Conference on Experimental Mechanics, Copenhagen, Denmark 2, 765-73.
Melvin, A.D., Lucia, A.C., Solomos, G., 1993. The thermal response to deformation to fracture of a carbon/epoxy composite laminate. Composites Science and Technology 46, 345-351.
Palumbo, D., De Finis, R., Demelio, P.G., Galietti, U., 2017. Early Detection of Damage Mechanisms in Composites During Fatigue Tests. Fracture, Fatigue, Failure and Damage Evolution 8, 133-141.
Risitano, A., D'Aveni, A., Fargione, G., Clienti, C., 2016. Identification of local phenomena of plasticity in concrete under compression test. Procedia Structural Integrity 2, 2123–2131.

Risitano, A., Risitano, G., 2013. Determining fatigue limits with thermal analysis of static traction tests. Fatigue & Fracture of Engineering Materials & Structures 36, 631-639.
Risitano, G., Clienti, C., 2012. Experimental study to verify the fatigue limit found by thermal analysis of specimen surface in mono axial traction test. Key Engineering Materials 488-489, 795-798.
Susmel, L., 2014. A unifying methodology to design un-notched plain and short fibre/particle reinforced concretes against fatigue. Int J Fatigue 61, 226–243
Thomas, C., Setién, J., Polanco, J.A., Lombillo, I., 2014. Fatigue limit of recycled aggregate concrete. Construction and Building Materials 52, 146–154.